UNIVERSITY OF AMSTERDAM

MSc Physics and Astronomy
Track: Astronomy & Astrophysics

Master Thesis

Title of Thesis

Subtitle of Thesis
Can use two lines

by

Karan Kumar
14906619(UVA)

December 16, 2024
60 ECTS
02-09-2024 - End date

Supervisors:
Lex Kaper
Daily Supervisor

Examiners
Alex De Koter

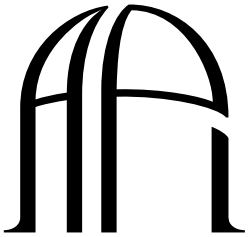

ANTON PANNEKOEK
INSTITUTE

Contents

List of Figures

List of Tables

List of Abbreviations

Chapter 1

Introduction

1.1 Introduction

High mass X-ray binaries (HMXBs) consist of a massive star O-type or B-type ($\geq 8M_{\odot}$) orbiting a compact X-ray source. Typically a neutron star or black hole. The X-rays are produced via accretion from the massive companion either by stellar wind mass loss or by Roche-Lobe overflow van den Heuvel et al. (2000). Runaways are formed when the binary system is ejected out of the galactic mid-plane or if the system has high peculiar velocity. ($\geq$20-30 km/s) Although this velocity isn't constrained to this limit CITE CITE CITE. Since their prediction by Blaauw (1961) HMXBs have been observed through various space telescopes the very first with *Hipparcos* Chevalier & Ilovaisky (1998); Moffat et al. (1998) and *Gaia* Carretero-Castrillo et al. (2023) CITE APPELANIZ. My project it to use *Gaia* DR3 to search for HMXB runaways and measure their space velocity and reconstruct the evolutionary history of the binary system. Gaia Collaboration et al. (2023)

1.1.1 GAIA Space Telescope by ESA

The *Gaia* space mission run by the European Space Agency provides astrometry of stars in the galaxy with great precision, It measures the position, proper motions and brightness of stars in the Galaxy, and is the successor to the *Hipparcos* space mission. *Hipparcos*, which ran from 1989 to 1993, measured the parallax (ω), right ascension (α), declination (δ), Proper Motion in Right Ascension(μ_{α}), and Proper Motion in declination (μ_{δ}) In literature this is known as 5-parameter astrometry Gaia Collaboration et al. (2023), CITE PERRYMAN 1997. *Hipparcos* was capable of measuring parallax with milliarcsecond precision and recorded 5-parameter astronomy solutions for 118,218 stars in the galaxy, All of the stars are avaliable in the *Hipparcos* Catagloue by CITE PERRYMAN 1997.

which was the first *Gaia* also classifies other parameters of stars such as effective temperature, metalicity and spectra. Since data release 3 (DR3) *Gaia* has mapped these parameters for over 1.8 billion sources with color magnitudes as faint as G=21 and up to as bright as G=3 Gaia Collaboration et al. (2023).DR3 was released 13 June 2022 and publicly available on the *Gaia* archive, which let's users search for any star on the catalogue for free. The catalogue by Neumann et al. (2023) XRBcats contains the data for all known HMXBS in the galaxy for both the compact object and the optical counterpart. We use XRBcats to find the optical counterpart in the *Gaia* archive. For each optical counterpart we obtain the position, proper motions, parallax and radial velocities (if available) to determine the peculiar velocity of each star.

1.1.2 History of HMXBs

O Stars and B stars are the most massive hydrogen burning stars in the Milky Way Also known as population I stars, these stars are the youngest in the galaxy which makes them important to understand metalicity and supernovae and star formation, in the Milky Way these regions are localized to the spiral arms Neumann et al. (2023). these stars were significant in determining the Oort constant for differential rotation in the galaxy Gies & Bolton (1986). Among the O and B stars, there are a number of stars that have significantly high space velocity and move away from their OB association, their velocity cannot be explained by redshift (CITE GIES AND BOLTON 1987) therefore their space velocity must come from another mechanism. In Blaauw (1961) surveyed 19 O-type and B-type stars with space velocity greater than 40km s^{-1} and classified these stars as runaways. Following the work by Blaauw (1961) further results define runaways as stars with large peculiar velocity, Far distance from the the galactic mid-plane or a combination of both.(Blaauw (1961); Carretero-Castrillo et al. (2023); de Wit et al. (2005)). Of the observed O-type stars in the galaxy, 30% are runways GIES 1987

1.1.3 Local Standard of Rest Frame

Consider a star at point S as show in figure 1.1. point S is somewhere in the galactic plane, with distance R from the galactic centre. It has 3-component velocity (Π, Θ,z) Π represents the velocity component which is positive towards the galactic centre, $\vec{CS}$, Θ represents the velocity positive in the direction of galactic rotation and Z represent the velocity above the mid-plane. This represents the total velocity of the star at point S, for a given time. The total velocity is comprised of 1.The star's peculiar velocity, 2.the velocity due to galactic rotation 3.Observational bias from the sun's motion in the galaxy. If the galactic center rotates with velocity θ_c then we

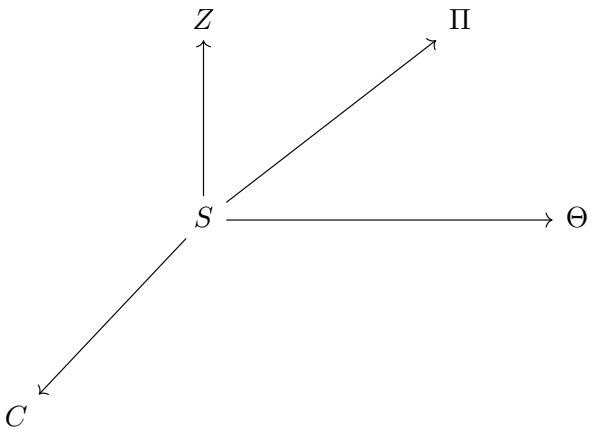

FIG. 1.1 – Local Standard of Rest Frame Delhaye (1965)

can reduce velocity of the star to it's local standard of rest frame (LSR) as

$$\vec{V_{lsr}} = [\Pi, \Theta - \Theta_c, Z]$$

Observationally, solar motion adds systematic error to the velocity since the sun is moving in the galactic plane as well, the true LSR velocity is therefore

$$\vec{V_{lsr}} = [\Pi - \Pi_\odot, \Theta - \Theta_c - \Theta_\odot, Z - Z_\odot]$$

Where $(\Pi_\odot, \Theta_\odot, Z_\odot)$ represent the solar motion components. The peculiar velocity is always measured with respect to the LSR frame Delhaye (1965). All stellar motion is reduced to FROM SOLAR MOTION WHEN APPLICABLE (FIX)

The Galactocentric distance is simply given by the law of cosine Brand & Blitz (1993), Moffat et al. (1998)

1.1.4 SuperNova Ejection Scenario

The compact object is a remenant of the most massive star in progenitor system called the primary star. As the more massive star it evolve much faster compared to the secondary star. During the core helium burning phase of the primary, the shell expands and mass transfer begins onto the primary via the secondary star Blaauw (1961), **?** At the end of it's lifetime the primary star allows explode into a Type II supernova becoming the compact the object.The roles are now switched the secondary now becomes the primary star in the system. The system can remain bound if less than half of the total mass of the system is lost during the supernova, CITE THIS. The energy of the supernova create the runaway velocity observed in HMXBs. van den Heuvel et al. (2000)

1.1.5 Dynamical Ejection Scenario

1.1.6 BeXray Binaries

Be X-Ray binaries consist of a compact object with a B-type emission companion star. Be-stars area a subgroup of B-type stars and are quite interesting to study as they have excited Balmer lines which generates emission Abt & Cardona (1984), Boubert & Evans (2018). Their emission comes from a circumstellar disk which is formed as a result of the rapid rotation of the Be-star around its axis Dufton et al. (2022). This circumstellar disk is also know as a deccretion disk which is also a source of infrared emissionCarretero-Castrillo et al. (2023). Be-stars may be a product of post-mass transfer systems Pols et al. (1991) in which a B-type star transfers mass into a companion, it is suggested that this post-mass transfer produces the deccretion disk in Be-stars therefore Be-stars may be a product of binary mass transfer, although the observational fraction of Be-stars in binary is poor Pols et al. (1991). This is paper THERE ARE N NUMBER OF Be-stars.

1.1.7 The Compact Object

Jeremy Orosz

1.2

Name	SpType	G	l	b	Parallax	distance	μ_l cos(b)	μ_b	$Vpec$	Mx
		mag	deg	deg	mas	kpc	mas/yr	mas/yr	km/s	$M_\odot$
1A 0535+262	O9.7IIIe	8.60	181.44	-2.64	0.53(0.0230)	1.91(0.0850)	2.13	-2.03	12.76	NaN
1A 1118-61	O9.5Ve	11.59	292.50	-0.89	0.33(0.0110)	3.04(0.1060)	-5.57	-0.51	13.18	NaN
1E 1145.1-6141	B2Iae	12.26	295.49	-0.01	0.13(0.0100)	7.89(0.6380)	-6.61	0.83	49.26	1.70
1ES 1210-64.6	B5V	13.98	298.89	-2.30	0.26(0.0180)	3.78(0.2530)	-5.96	-0.38	6.14	NaN
1FGL J1018.6-5856	O6V((f))	12.27	284.35	-1.69	0.23(0.0100)	4.40(0.1980)	-6.65	-1.59	28.33	2.00
1H 2202+501	B3e	9.30	97.25	-4.04	0.88(0.0130)	1.14(0.0170)	1.73	-1.64	24.95	NaN
2S 0114+650	B1Iae	10.52	125.71	2.56	0.20(0.0110)	5.09(0.2920)	-1.32	0.62	20.31	NaN
3U 1223-62	B1 Ia+	9.75	300.10	-0.04	0.25(0.0160)	3.99(0.2550)	-5.03	-2.52	46.23	NaN
3U 1258-61	B2 Vne	12.65	304.10	1.25	0.54(0.0140)	1.85(0.0480)	-4.35	-0.03	18.95	NaN
4U 0115+63	B0.2Ve	14.30	125.92	1.03	0.14(0.0160)	7.34(0.8800)	-1.73	0.31	21.92	NaN
4U 0352+309	B0Ve	6.26	163.08	-17.14	1.63(0.0370)	0.61(0.0140)	0.31	-2.25	14.03	NaN
4U 0728-25	O5Ve	11.60	240.28	-4.05	0.10(0.0170)	10.44(1.8650)	-1.99	0.09	9.27	NaN
4U 1145-619	B0.2 III	8.65	295.61	-0.24	0.47(0.0170)	2.10(0.0770)	-6.43	0.10	8.98	NaN
4U 1538-52	B0 Iab	13.16	327.42	2.16	0.13(0.0150)	7.82(0.9320)	-7.83	0.83	66.08	NaN
4U 1954+31	M4 I	8.36	68.39	1.93	0.26(0.0240)	3.88(0.3690)	-6.30	-1.35	25.84	NaN
4U 2206+54	O9.5IIIe	9.74	100.60	-1.11	0.30(0.0140)	3.28(0.1460)	-5.32	-0.32	26.16	NaN
AX J1700.2-4220	B2e	8.71	343.80	-0.03	0.64(0.0230)	1.56(0.0560)	-0.44	-1.83	18.07	NaN
AX J1845.0-0433	O9.5I	12.76	28.14	-0.66	0.16(0.0240)	6.10(0.8810)	-5.60	-1.36	46.70	NaN
BSD 24-491	B0e	10.40	159.85	-1.27	0.38(0.0150)	2.64(0.1050)	0.96	-0.70	1.44	NaN
CCDM J07474-5320A	B7 IV-Ve	7.54	266.31	-13.73	1.54(0.0210)	0.65(0.0090)	-9.68	-0.06	4.80	NaN
Cen X-3	O6.5 II-III	12.88	292.09	0.34	0.14(0.0140)	7.21(0.7120)	-3.72	1.16	85.15	1.34
Cep X-4	B1-B2Ve	13.82	99.01	3.31	0.10(0.0130)	9.54(1.1520)	-3.68	0.27	42.12	NaN
Cyg X-1	O9.7Iabpvar	8.54	71.33	3.07	0.44(0.0150)	2.25(0.0760)	-7.37	-0.10	27.64	21.20
GRO J1008-57	B0 IIIVe	13.88	283.00	-1.82	0.24(0.0130)	4.12(0.2240)	-5.89	0.25	13.02	NaN
GRO J2058+42	O9.5-B0IV-Ve	14.13	83.57	-2.65	0.08(0.0150)	12.90(2.5350)	-3.98	-0.56	52.48	NaN
Ginga 0834-430	B0-2III-Ve	19.15	262.02	-1.51	1.10(0.2170)	0.91(0.1780)	-4.95	-0.28	11.55	NaN

HD 110432	B0.5IVpe	5.14	301.96	-0.20	2.28(0.0770)	0.44(0.0150)	-12.77	-3.98	1.78	NaN
HD 119682	B0Ve	8.52	309.15	-0.72	0.60(0.0290)	1.65(0.0780)	-5.13	-1.16	7.78	NaN
HD 141926	B2 IIIn	8.69	326.98	-1.24	0.73(0.0180)	1.37(0.0340)	-4.46	-0.46	5.22	NaN
HD 153919	O6Iafcp	6.42	347.75	2.17	0.63(0.0260)	1.58(0.0650)	5.46	1.11	60.92	NaN
HD 161103	B0.5 III-Ve	8.23	1.36	1.05	0.79(0.0240)	1.27(0.0380)	-2.41	-0.47	4.74	NaN
HD 215227	B1.5-B2III	8.71	100.17	-12.40	0.49(0.0180)	2.06(0.0780)	-4.56	-1.13	10.30	NaN
HD 249179	B5ne	10.01	181.28	1.86	0.60(0.0300)	1.67(0.0840)	2.21	-0.55	5.54	NaN
HD 34921	B0 IVpe	7.23	170.05	0.71	0.72(0.0300)	1.39(0.0580)	4.04	-1.18	12.13	NaN
HD 77581	B0.5 Ib	6.74	263.06	3.93	0.50(0.0150)	2.02(0.0620)	-10.13	2.61	52.43	NaN
HD 96670	O8.5f(n)p	7.35	290.20	0.40	0.31(0.0280)	3.22(0.2910)	-6.88	-1.01	10.09	6.20
HESS J0632+057	B0Vpe	8.88	205.67	-1.44	0.54(0.0230)	1.85(0.0780)	0.37	-0.22	5.47	NaN
HR 4804	B8Vn(e)	6.54	302.14	-12.52	4.77(0.0270)	0.21(0.0010)	-26.97	-9.99	7.20	NaN
IGR J00370+6122	BN0.5II-III / BN0.7Ib	9.46	121.22	-1.46	0.27(0.0120)	3.68(0.1630)	-1.82	-0.44	1.92	NaN
IGR J01363+6610	B1Ve	12.46	127.39	3.73	0.17(0.0110)	5.99(0.3940)	-1.59	-0.32	9.42	NaN
IGR J01583+6713	B2IVe	13.69	129.35	5.19	0.13(0.0130)	7.50(0.7400)	-1.24	-0.03	4.25	NaN
IGR J06074+2205	B0.5Ve	12.17	188.38	0.81	0.14(0.0180)	7.24(0.9470)	0.81	0.20	23.13	NaN
IGR J08262-3736	OBV	12.16	256.44	0.28	0.18(0.0100)	5.63(0.3060)	-3.96	-0.05	6.70	NaN
IGR J08408-4503	O8.5Ib-II(f)p	7.45	264.04	-1.95	0.44(0.0170)	2.26(0.0860)	-9.41	-2.08	40.72	NaN
IGR J11215-5952	B0.5Ia	9.77	291.89	1.07	0.12(0.0120)	8.11(0.8110)	-5.76	0.88	42.47	NaN
IGR J11305-6256	B0IIIne	8.13	293.94	-1.49	0.57(0.0470)	1.75(0.1420)	-6.23	-0.49	7.02	NaN
IGR J16195-4945	ON9.7Iab	16.37	333.56	0.34	0.36(0.0510)	2.79(0.3920)	-0.52	-0.26	34.32	NaN
IGR J16465-4507	B0.5-1Ib	13.48	340.05	0.14	0.30(0.0170)	3.38(0.1970)	-3.48	-0.63	18.82	NaN
IGR J17544-2619	O9Ib	11.66	3.24	-0.34	0.40(0.0270)	2.52(0.1700)	-0.83	0.10	9.44	1.40
IGR J18406-0539	B5V	11.23	26.66	-0.23	0.23(0.0150)	4.30(0.2690)	-3.08	-0.45	3.22	NaN
IGR J18462-0223	NaN	17.65	30.22	0.08	0.68(0.1210)	1.48(0.2640)	-2.65	0.43	10.63	NaN
IGR J21343+4738	B1–1.5III–V	14.00	92.17	-3.12	0.08(0.0140)	11.97(2.0300)	-3.35	-0.43	30.81	NaN
LS 1698	B0V-IIIe	11.24	285.35	1.43	0.17(0.0160)	5.84(0.5540)	-6.97	-0.40	32.74	NaN
LS 5039	ON6V((f))z	10.80	16.88	-1.29	0.49(0.0150)	2.04(0.0630)	-3.73	-10.38	94.91	NaN
LS 992	B0.2IVe	12.42	249.58	1.54	0.12(0.0120)	8.45(0.8750)	-2.59	-0.01	11.06	NaN

LS I +61 303	B0Ve	10.40	135.68	1.09	0.38(0.0130)	2.65(0.0910)	-0.28	-0.41	4.17	NaN
MAXI J0709-159	NaN	9.19	229.31	-3.36	0.32(0.0240)	3.17(0.2440)	-2.06	-0.99	10.59	NaN
MXB 0656-072	O9.7Ve	11.98	220.13	-1.77	0.15(0.0150)	6.50(0.6400)	-1.41	0.01	13.58	NaN
NGC 6649 9	B0Ve	10.96	21.64	-0.79	0.47(0.0280)	2.11(0.1250)	-0.09	-0.06	20.05	NaN
PSR B1259-63	O9.5Ve	9.63	304.18	-0.99	0.44(0.0130)	2.25(0.0680)	-7.10	0.04	12.99	NaN
PSR J0635+0533	B1IIIe-B2Ve	12.50	206.15	-1.04	0.14(0.0150)	7.02(0.7350)	-0.55	-0.18	10.19	NaN
PSR J2032+4127	B0:e/B0:Vn	11.28	80.22	1.03	0.57(0.0160)	1.76(0.0480)	-2.49	1.73	27.43	NaN
RX J0146.9+6121	B1III-Ve	11.21	129.54	-0.80	0.33(0.0220)	3.05(0.2010)	-0.99	-0.31	4.52	NaN
SAO 49725	B0.5III-Ve	9.03	85.23	5.05	0.42(0.0160)	2.38(0.0910)	-5.26	-0.51	8.06	NaN
SAX J2103.5+4545	B0Ve	13.77	87.13	-0.69	0.13(0.0130)	7.64(0.7560)	-4.70	0.46	36.70	NaN
SAX J2239.3+6116	B0Ve	14.11	107.73	2.36	0.10(0.0140)	9.62(1.2920)	-2.54	0.22	19.68	NaN
SGR 0755-2933	B0Ve	9.94	246.23	-0.61	0.28(0.0140)	3.50(0.1710)	-3.86	-0.73	5.56	1.40
SRGA J124404.1-632232	Be	15.08	302.11	-0.52	0.12(0.0220)	8.11(1.4580)	-6.35	-0.42	15.15	NaN
SS 397	B0.5Ve	11.72	21.47	-0.87	1.08(0.1940)	0.93(0.1670)	-0.10	-1.11	12.36	NaN
SS 433	A3-7 I	12.60	39.69	-2.25	0.12(0.0230)	8.46(1.6660)	-5.64	0.45	31.01	4.20
Swift J0243.6+6124	O9.5Ve	12.39	135.93	1.43	0.18(0.0110)	5.51(0.3440)	-0.72	-0.19	2.38	NaN
TYC 3681-695-1	B1-2 III/Ve	11.41	126.08	-3.57	0.34(0.0180)	2.95(0.1570)	-2.39	-0.80	13.26	NaN
V0332+53	O8-9Ve	14.20	146.05	-2.19	0.13(0.0200)	7.44(1.1160)	-0.48	0.20	18.23	NaN
XTE J0421+560	B1/2I[e]	10.77	149.18	4.13	0.21(0.0150)	4.76(0.3370)	0.03	-0.69	10.76	NaN
XTE J1739-302	O8Iab(f)	12.64	358.07	0.45	0.52(0.0480)	1.94(0.1800)	2.96	2.36	50.50	NaN
mu.02 Cru	B5Vne	5.15	303.37	5.70	8.27(0.1170)	0.12(0.0020)	-28.61	-9.82	3.28	NaN

Bibliography

Abt H. A., Cardona O., 1984, , 285, 190

Blaauw A., 1961, , 15, 265

Boubert D., Evans N. W., 2018, , 477, 5261

Brand J., Blitz L., 1993, , 275, 67

Carretero-Castrillo M., Ribó M., Paredes J. M., 2023, , 679, A109

Chevalier C., Ilovaisky S. A., 1998, , 330, 201

Delhaye J., 1965, in Blaauw A., Schmidt M., eds, , Galactic structure. Edited by Adriaan Blaauw and Maarten Schmidt.. University of Chicago Press, p. 61

Dufton P. L., Lennon D. J., Villaseñor J. I., Howarth I. D., Evans C. J., de Mink S. E., Sana H., Taylor W. D., 2022, , 512, 3331

Gaia Collaboration et al., 2023, , 674, A1

Gies D. R., Bolton C. T., 1986, , 61, 419

Moffat A. F. J., et al., 1998, , 331, 949

Neumann M., Avakyan A., Doroshenko V., Santangelo A., 2023, , 677, A134

Pols O. R., Cote J., Waters L. B. F. M., Heise J., 1991, , 241, 419

de Wit W. J., Testi L., Palla F., Zinnecker H., 2005, , 437, 247

van den Heuvel E. P. J., Portegies Zwart S. F., Bhattacharya D., Kaper L., 2000, , 364, 563